

Shaping the $g^{(2)}$ autocorrelation and photon statistics

Ivo Straka* and Miroslav Ježek

Department of Optics, Faculty of Science, Palacký University, 17. listopadu 12, 771 46, Olomouc, Czechia

We propose a method of arbitrarily shaping and scaling the temporal intensity correlations of an optical signal locally, i.e. avoiding periodic correlations. We demonstrate our approach experimentally using stochastic intensity modulation. We also propose shaping both temporal correlations and photon statistics using the methods published by [Pandey et al., EPJ Plus 129, 115 (2014)] and [Straka et al., Opt. Express 26, 8998 (2018)].

I. INTRODUCTION

This letter focuses on temporal correlations of optical intensity $I(t)$, conventionally described by the second-order coherence function

$$g^{(2)}(\tau) = \frac{\langle I(t)I(t+\tau) \rangle}{\langle I(t) \rangle^2} \quad (1)$$

which we refer to as intensity autocorrelation. In the quantum realm, it is defined by the means of normally ordered photon-number operators [1]

$$g^{(2)}(\tau) = \frac{\langle : \hat{n}(t) \hat{n}(t+\tau) : \rangle}{\langle \hat{n}(t) \rangle^2}. \quad (2)$$

This letter proposes methods of shaping the autocorrelation $g^{(2)}(\tau)$ in an arbitrary way. A straightforward approach would be modulating a pulse train coming from a laser, however pulsed signals have periodic autocorrelation. Our goal is to emulate fluctuating signals exhibiting $g^{(2)}(0) \geq 1$ that approaches unity in the limit of $\tau \rightarrow \infty$. Any significant deviation from unity is therefore local.

The modulation of optical intensity in time can be used to generate pseudo-thermal light. A common technique is collecting speckles from light diffused by a rotating ground glass plate [2]. The resulting photon bunching of $g^{(2)}(0) \geq 2$ can be exploited in classical ghost imaging [3].

Shaping the autocorrelation—and thus, the spectrum—of a signal is a problem that has been addressed in other fields of signal processing/simulation using various methods [4, 5]. A prominent case is transforming an electronic Gaussian noise by a linear filter and a nonlinear function to obtain a given spectrum and marginal distribution [6]. An alternate solution was proposed in terms of reshuffling of signal samples [7].

In the first part of this letter, we present a method of shaping the autocorrelation that exploits stochastic pulse superposition. The spectral properties of such random pulses have been studied in communication theory [8]; we make use of these properties from the perspective of signal generation.

In the second part, we utilize another method of stochastic modulation proposed in Ref. [9] to shape both

temporal correlations and photon statistics. Our contribution is combining the published method [9] with the photon-statistics-generation algorithm proposed in Ref. [10], providing simulations, and analysing the method's properties and limitations.

II. ARBITRARY AUTOCORRELATION

A. Method

The basic premise is that the intensity signal $I(t)$ consists of a random Poissonian sequence of non-negative integrable hill functions $h(t)$. Mathematically, the signal is expressed as a sum

$$I(t) = \sum_i h(t - t_i). \quad (3)$$

The sequence of positions in time $\{t_i\}$ is a homogeneous Poisson point process with a mean rate λ . This means that every delay $\Delta t_i = t_{i+1} - t_i$ is a realization of a random variable with a probability density

$$p(\Delta t) = \lambda \exp(-\lambda \Delta t). \quad (4)$$

The hill function is chosen so that it has a specific cross-correlation $C(\tau)$, while its L^1 norm $\|h\|$ may be arbitrary. The terms are defined as

$$\|h\| := \int_{-\infty}^{\infty} h(t) dt, \quad (5)$$

$$C(\tau) := \frac{1}{\|h\|^2} \int_{-\infty}^{\infty} h(t+\tau)h(t) dt, \quad (6)$$

where the cross-correlation is normalized; $\int_{-\infty}^{\infty} C(\tau) d\tau = 1$. Then, the intensity autocorrelation of $I(t)$ becomes

$$g^{(2)}(\tau) = 1 + \frac{1}{\lambda} C(\tau). \quad (7)$$

The proof is given in Appendix B. The autocorrelation shape is therefore given solely by the shape of $h(t)$, the amplitude of which may be arbitrary. The $g^{(2)}(0)$ and the scale of the whole autocorrelation can be set by the rate λ .

* straka@optics.upol.cz

Given a specific $g^{(2)}(\tau)$, one can obtain the hill function using Fourier transforms \mathcal{F} ,

$$h(t) = \mathcal{F}^{-1} \left(\pm \sqrt{\mathcal{F} [g^{(2)}(\tau) - 1]} \right), \quad (8)$$

where the \pm element is an arbitrary piecewise sign function. The $g^{(2)}(\tau)$ needs to be given so that both Fourier transforms in (8) yield non-negative functions.

a. Superposition A generalization of this approach allows generating a superposition of multiple shapes by randomly alternating between hill functions. Suppose a set of hill functions $\{h_n(t)\}$ with respective cross-correlations $C_n(\tau)$ appearing with probabilities p_n , but sharing the same frequency λ . The calculation of $g^{(2)}(\tau)$ is a straightforward extension, yielding

$$g_{\text{mul}}^{(2)}(\tau) = 1 + \frac{1}{\lambda} \frac{\sum_n p_n C_n(\tau)}{(\sum_n p_n \|h\|_n)^2}. \quad (9)$$

b. Background If we consider a background offset I_{bg} so that $I(t) = \sum_i h(t - t_i) + I_{\text{bg}}$, the mean value of the signal is $\langle I(t) \rangle = \lambda \|h\| + I_{\text{bg}}$ and the signal-to-noise ratio between $\|h\|$ and I_{bg} becomes a factor that scales down the intensity autocorrelation:

$$g_{\text{bg}}^{(2)}(\tau) = 1 + \frac{C(\tau)}{\lambda \left(1 + \frac{I_{\text{bg}}}{\lambda \|h\|}\right)^2}. \quad (10)$$

The maximum bunching $g^{(2)}(0)$ is achieved for $\lambda = I_{\text{bg}}/\|h\|$.

c. Non-overlapping hills In a particular experimental realization—such as presented here—it may not be possible to generate a mathematical superposition of the hill functions. For example, a function generator can only produce one pulse at a time and so the hills cannot overlap. In such cases, the hill function is defined on a finite support $t \in (-t_0/2, t_0/2)$ and the minimum distance between the hills' peaks is t_0 . Consequently, the cross-correlation $C(\tau)$ is only nonzero for $\tau \in (-t_0, t_0)$, and the unity term in (7) becomes locally distorted. The expression changes to

$$g_{\text{non-ol}}^{(2)}(\tau) = \left(\frac{1}{\lambda} + t_0 \right) C(\tau) + (1 + \lambda t_0) \times \sum_{k=0}^{\lfloor |\tau|/t_0 \rfloor} \int_{t=0}^{|\tau| - kt_0} \left[C(\tau + t + (k+1)t_0) + C(\tau - t - (k+1)t_0) \right] \lambda^k \frac{t^k}{k!} e^{-\lambda t} dt. \quad (11)$$

B. Results

The method of stochastic signal generation is simulated in Fig. 1. For illustrative purposes, the signals are shown for both high and low intensities λ , respectively

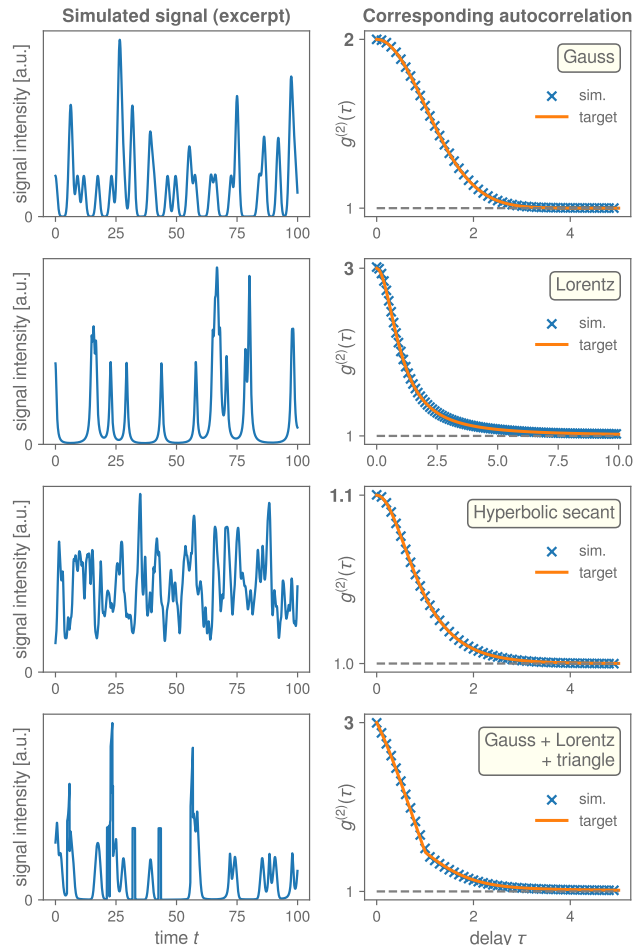


FIG. 1. Monte-Carlo simulations of signals with various prescribed autocorrelation shapes and values of $g^{(2)}(0)$. [11]

corresponding to low and high values of $g^{(2)}(0)$. A mixture of three shapes corresponding to (9) is given in the last row.

Experimental evidence was obtained using the measurement setup is depicted in Fig. 2. The source was a single-mode-fiber-coupled (SMF) continuous-wave laser diode at 814 nm. The optical signal was coupled into a polarization-maintaining fiber (PMF) using a manual polarization controller and a polarizing beam splitter (PBS). The intensity of the signal was modulated by an integrated electro-optical Mach-Zehnder modulator (EOM; EOSpace). The modulator was driven by an arbitrary signal generator (Tektronix) programmed to emit a voltage pulse upon each triggering event, which was fed into the fast radio-frequency input of the EOM, having the shape

$$V(t) = \frac{V_\pi}{\pi} \arccos[1 - 2h(t)], \quad (12)$$

where the hill is scaled so that $h(t) \in [0, 1]$, and V_π is the EOM half-wave voltage. The induced transmission modulation is equal to $h(t)$ due to the cosine response of the

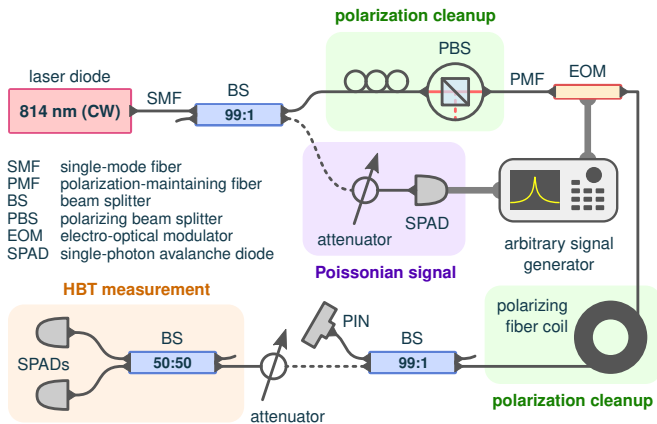


FIG. 2. The measurement scheme with the data given in Fig. 3.

EOM. We assume that the constant bias voltage of the EOM is set precisely to the zero-level transmission. The triggering came from a single-photon avalanche diode (SPAD) illuminated by a constant intensity that was set to a mean count rate λ . This served as the source of Poissonian events. The output was split between a PIN diode and a single-photon Hanbury-Brown-Twiss (HBT) measurement [1]. The PIN served for live monitoring of the output and the HBT configuration measured the $g^{(2)}(\tau)$. For all measurements, the minimum pulse-to-pulse delay was $t_0 \geq 3 \mu\text{s}$. It means that the triggering SPAD dead time of 29 ns could be safely neglected. The data from the SPADs were acquired by a 81-ps time-tagging unit (qtools), the coincidence window for the HBT autocorrelation measurement was 10 ns, and the measurement time was 100 s for each set.

The results of the HBT measurement are shown in Fig. 3. The Gaussian autocorrelation was set to the highest possible amplitude of $g^{(2)}(0) = 214$, corresponding to a modulation dynamic range 30.8 dB, while the others were set to round values 50, 100, and 150. The modulation scheme corresponds to the non-overlapping scenario with the expected autocorrelation given by (11), where the effect of non-unity background is small compared to the overall amplitude [11].

The limiting factor for the autocorrelation amplitude is the EOM dynamic range. It is reduced by thermally induced phase drifts in the EOM, by the polarization extinction ratio, and by the EOM interferometric visibility. The limiting factor for speed is the 225-MHz bandwidth of the arbitrary signal generator.

III. PHOTON STATISTICS AND AUTOCORRELATION

There is a possibility of tailoring both temporal autocorrelation and photon (intensity) statistics simultaneously and independently. The technique relies on random switching between intensity levels. This approach was

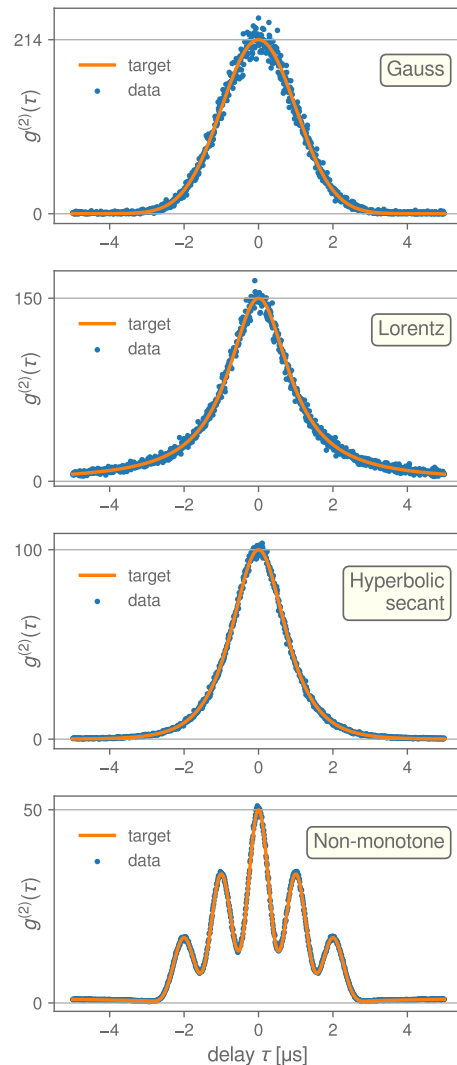


FIG. 3. The autocorrelation functions measured with the HBT configuration. The good match between the prescribed orange curves and the data was achieved, by generating the voltage pulses of the appropriate shape, by tuning the Poissonian trigger rate λ , and by setting the EOM bias voltage as precisely as possible. All data and code are available online [11].

proposed by Pandey et al. [9] who demonstrated the generation of various photon statistics and autocorrelation shapes. Here we shall combine it with a photon-statistics inversion algorithm proposed in our earlier work [10]. We present an analysis of the combined methods' limitations and we perform numerical simulations [11].

The optical signal consists of a sequence of intensity levels $\{I_i\}$, each being held for a respective time period $\{\Delta t_i\}$. Each I_i and Δt_i is an independent realization of the corresponding random variable, following the probability density distributions $p(I)$ and $p(\Delta t)$.

The autocorrelation is then given as [9] (see Ap-

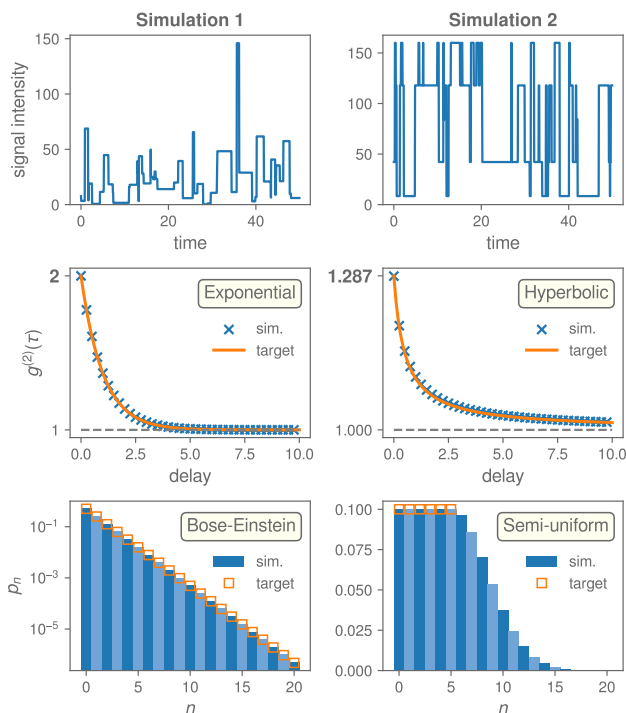


FIG. 4. Numerical simulations of signals having prescribed autocorrelations and photon statistics. Signal excerpts are shown in the top row; autocorrelations in the middle row; photon statistics per window $T = 0.05$ are shown at the bottom. [11]

pendix E)

$$g^{(2)}(\tau) = 1 + \frac{g^{(2)}(0) - 1}{\langle \Delta t \rangle} \int_{\tau}^{\infty} p(\Delta t)(\Delta t - \tau) d\Delta t, \quad (13)$$

$$g^{(2)}(0) = \frac{\langle I^2 \rangle}{\langle I \rangle^2}. \quad (14)$$

The averaging terms $\langle \cdot \rangle$ are always taken over the corresponding distributions – $p(I)$ or $p(\Delta t)$. The bunching factor (14) is solely given by intensity statistics – as it needs to be – while the temporal shape is given by $p(\Delta t)$. To establish the set of possible $g^{(2)}$ shapes, let us look at the derivative

$$\frac{dg^{(2)}(\tau)}{d\tau} = -\frac{g^{(2)}(0) - 1}{\langle \Delta t \rangle} \int_{\tau}^{\infty} p(\Delta t) d\Delta t. \quad (15)$$

The right-hand side of (15) is proportional to the survival function of Δt , which is a monotonically non-increasing function that begins at 1 ($\tau = 0$) and approaches 0 ($\tau \rightarrow \infty$). At the same time, *any* function that has these properties can be considered a survival function and therefore defines a valid modulation process governed by $p(\Delta t)$. The pre-integral factor in (15) is negative, which means that the autocorrelation slope needs to be negative and monotonically non-decreasing (i.e. $d^2g^{(2)}(\tau)/d\tau^2 > 0$, implying convexity). We can therefore conclude that the class of practicable autocorrelation

functions is restricted to monotonically non-increasing convex functions for which the limit $\lim_{\tau \rightarrow \infty} g^{(2)}(\tau) \rightarrow 1$. This is more restrictive than the hill-superposition approach above, as for example all functions in Figs. 1, 3 are non-convex and therefore inaccessible. However, we gain the possibility to shape the photon statistics independently.

Photon statistics is given by the integrated intensity

$$W(t) = \int_t^{t+T} I(t') dt', \quad (16)$$

taken over a time interval T [12]. Let us consider the units of $I(t)$ to be the average number of photons per time, meaning that W is dimensionless. The number of photons n detected inside a time interval follows the probability distribution given by Mandel's formula [12]

$$p(n) = \int_0^{\infty} p(W) \frac{W^n}{n!} e^{-W} dW. \quad (17)$$

In order to have control over the photon statistics, the distribution $p(W)$ needs to follow $p(I)$, ideally when $W(t) = T \times I(t)$, implying $p(W) = p(I)/T$. This can be achieved either in the limit of a short time window $T \rightarrow 0$, or if the intensity switching is synchronized with the time windows. The latter implies that the window length T becomes an elementary time unit of the modulation, and the autocorrelation is restricted to a piecewise linear function with the resolution T . This case corresponds to our discrete numerical simulations.

Following the approach presented in [10], we take a finite set $\{W_k\}$ and form a matrix $A_{nk} = \exp(-W_k) W_k^n / n!$. Each W_k has a corresponding probability P_k . The Mandel formula (17) then becomes

$$p(n) = \sum_k A_{nk} P_k, \quad (18)$$

where the vector P_k needs to be solved for a given photon statistics $p(n)$. Suitable sampling and non-negative-least-squares were shown to work for classical photon statistics [10, 11]. The solution for $p(I)$ is discrete: $\Pr[I = W_k/T] = P_k$.

Fig. 4 shows two numerically simulated signals that follow certain prescribed autocorrelations and photon statistics. Both signals observe their corresponding $p(\Delta t)$, but have different approaches to $p(I)$. Signal 1 takes samples from a continuous exponential distribution, whereas Signal 2 follows a discrete solution of (18) for a partially uniform photon statistics $p(n) = 0.1 \forall n \leq 5$.

IV. CONCLUSION

We demonstrated two methods of shaping the autocorrelation of optical intensity. The first allows for more arbitrary shapes; the second is limited to non-increasing convex functions, but allows tailoring the intensity/photon statistics as well.

While we consider our contribution to address a fundamental problem in optical signal generation, possible practical uses involve exciting or probing systems sensitive to photon correlations [13, 14]. The modulation techniques may also serve to simulate optical fading channels and atmospheric scintillation [15], especially if certain power spectra are required [16–18]. Atmospheric turbulence has a critical impact on satellite-based quantum communications [19, 20].

Appendix A: Data, code and tables

All resources are available online on CodeOcean, <https://doi.org/10.24433/CO.4221408.v1>.

The online capsule provides the measurement data, the software necessary to process them, and all simulations presented in the manuscript. From data and code, Figures 1, 2, 4 are generated.

Explicit definitions pertaining to the aforementioned Figures are listed in Tables I and II.

Appendix B: Derivation: autocorrelation of stochastic hill superposition

Let the “hill” function be $h(t)$ and its unnormalized cross-correlation function

$$CC(\tau) := (h \star h)(\tau) = \int_{-\infty}^{\infty} h(t)h(t+\tau)dt. \quad (\text{B1})$$

We are going to consider the intensity of light as a sum of hills randomly distributed in time:

$$I(t) = \sum_i h(t - t_i), \quad (\text{B2})$$

where the peaks t_i follow a homogeneous Poisson point process in time with a mean frequency λ . This means that peak-to-peak distances $\Delta t_i = t_{i+1} - t_i$ follow a negative-exponential probability density distribution $p(\Delta t_i) = \lambda \exp(-\lambda \Delta t_i)$. The normalized intensity autocorrelation function is

$$g^{(2)}(\tau) = \frac{\langle I(t)I(t+\tau) \rangle}{\langle I(t) \rangle \langle I(t+\tau) \rangle}. \quad (\text{B3})$$

Let us consider that the intensity signal was generated in a time span T and assume the limit of long T in our calculations. Then, the number of hills is $N \simeq \lambda T$. We can also denote the integral

$$\|h\| := \int_{-\infty}^{\infty} h(t)dt, \quad (\text{B4})$$

which also means $\int_{-\infty}^{\infty} CC(\tau)d\tau = \|h\|^2$. The averaging terms can be calculated simply using the linearity of

integration,

$$\begin{aligned} \langle I(t) \rangle &= \langle I(t+\tau) \rangle \\ &= \frac{1}{T} \int_T I(t)dt \simeq \frac{N\|h\|}{T}, \end{aligned} \quad (\text{B5})$$

$$\begin{aligned} \langle I(t)I(t+\tau) \rangle &= \frac{1}{T} \int_T \left(\sum_{i=1}^N h(t-t_i) \right) \\ &\quad \times \left(\sum_{j=1}^N h(t-t_j+\tau) \right) \\ &\simeq \frac{1}{T} \sum_{i,j} CC(\Delta t_{ij} + \tau), \end{aligned} \quad (\text{B6})$$

where $\Delta t_{ij} = t_j - t_i$ are distances between any two peaks – different or identical. The sum has N^2 terms that can be reduced by considering $\Delta t_{i=j} = 0$ and $\Delta t_{ij} = -\Delta t_{ji}$:

$$\begin{aligned} \frac{1}{T} \sum_{i,j} CC(\Delta t_{ij} + \tau) &= \frac{1}{T} \sum_{i < j} \left[CC(\tau + \Delta t_{ij}) \right. \\ &\quad \left. + CC(\tau - \Delta t_{ij}) \right] + \frac{N}{T} CC(\tau). \end{aligned} \quad (\text{B7})$$

The peak locations t_i are determined by sampling a random Poisson process and we sum over a large set of samples Δt_{ij} . We can therefore approximate the above sum by

$$\sum_{j=2}^N \sum_{i=1}^{j-1} CC(\tau \pm \Delta t_{ij}) \simeq \frac{N^2 - N}{2} \langle CC(\tau \pm \Delta t) \rangle_{\Delta t}, \quad (\text{B8})$$

where the averaging follows a certain probability distribution of distances Δt between any two different peaks. Let us now calculate this distribution. By virtue of the homogeneous Poisson process, we may consider any two different points in time independent with respect to the random occurrence of samples. This allows us to define the average density of peaks per time, which is constant: $\rho(0 < t < T) = \lambda$. Then, the density of peak pairs per distance Δt is

$$\rho_2(\Delta t) = \int_0^{T-\Delta t} \rho(t)\rho(t+\Delta t)dt = \lambda^2(T - \Delta t), \quad (\text{B9})$$

while the corresponding probability density distribution follows by normalizing

$$p(\Delta t) = \frac{\rho_2(\Delta t)}{\int_0^T \rho_2(\Delta t)d\Delta t} = \frac{2}{T} - \frac{2}{T^2}\Delta t. \quad (\text{B10})$$

Now we can make use of this distribution to calculate (B8). Because we assume that time T is much longer than both the width of CC and delay τ , we can either neglect the linear term in (B10) or integrate per-partes and approximate the primitive function of CC by a step function. In any way, we get

Shape	$C(\tau)$	$h(t)$	$g^{(2)}(0)$	λ
Gauss	$\frac{1}{\sqrt{2\pi}}e^{-\tau^2/2}$	$\frac{1}{\sqrt{\pi}}e^{-t^2}$	2	$\frac{1}{\sqrt{2\pi}}$
Cauchy-Lorentz	$\frac{1}{\pi(1+\tau^2)}$	$\frac{2}{\pi(1+4t^2)}$	3	$\frac{1}{2\pi}$
Hyperb. secant	$\frac{1}{2} \operatorname{sech} \frac{\pi\tau}{2}$	$\mathcal{F}^{-1} \left(\sqrt{\operatorname{sech}(2\pi\nu)} \right)$	1.1	5
Gauss + Lorentz + triangle	$\frac{1}{3} \frac{1}{\sqrt{2\pi}} e^{-\tau^2/2}$ $+ \frac{1}{3} \frac{1}{\pi(1+\tau^2)}$ $+ \frac{1}{3} \operatorname{tri}(-1, 1)$	$h_1(t) = \frac{1}{\sqrt{\pi}} e^{-t^2}$ $h_2(t) = \frac{2}{\pi(1+4t^2)}$ $h_3(t) = \operatorname{rect}(-\frac{1}{2}, \frac{1}{2})$	3	$\frac{1}{6} \left(1 + \frac{1}{\pi} + \frac{1}{\sqrt{2\pi}} \right)$
Non-monotone	$\frac{3- \tau }{18} [2 + \cos(2\pi\tau)]$ $+ \frac{1}{12\pi} \sin(2\pi \tau)$ for $ \tau < 3$	$\frac{1}{2} - \frac{1}{2} \cos(2\pi t)$ for $0 < t < 3$		

TABLE I. Table of autocorrelation shapes used in Fig. 1 of the manuscript. Fig. 2 uses the same shapes and the non-monotone shape, which is defined at the bottom. The functions $\operatorname{rect}()$ and $\operatorname{tri}()$ are rectangular and triangular functions of unit height and given edges.

	$g^{(2)}(\tau)$	p_n
Simulation 1	$1 + e^{- \tau }$	0.5^{n+1}
Simulation 2	$1 + 0.287 \frac{1}{2^{ \tau +1}}$	$p_{0,1,\dots,5} = 0.1$

TABLE II. Table of autocorrelation shapes and photon-number distributions used in Fig. 4.

$$\langle \operatorname{CC}(\tau + \Delta t) + \operatorname{CC}(\tau - \Delta t) \rangle_{\Delta t} \simeq \frac{2 \|h\|^2}{T}. \quad (\text{B11})$$

Now we can consecutively substitute (B11), (B8), (B7), use $N^2 \gg N$, and get

$$\langle I(t)I(t + \tau) \rangle \simeq \lambda \operatorname{CC}(\tau) + \frac{N^2 \|h\|^2}{T^2}. \quad (\text{B12})$$

Finally, after substituting the rest, we get the final result for the normalized autocorrelation of the randomly generated signal

$$g^{(2)}(\tau) = 1 + \frac{1}{\lambda} C(\tau), \quad (\text{B13})$$

where $C(\tau) = \operatorname{CC}(\tau)/\|h\|^2$ is the normalized cross-correlation of $h(t)$. We can see that the shape of $g^{(2)}(\tau)$ does not depend on the amplitude of $h(t)$, only on its shape. The scaling of the $g^{(2)}(\tau)$ is determined solely by the mean frequency λ .

Appendix C: Obtaining the hill shape from autocorrelation

Let us have a given autocorrelation function by specifying (B13) numerically or analytically. Our task is to determine $h(t)$ and λ , which together define the desired signal. We use the property of the Fourier transform of a cross-correlation, $\mathcal{F}(\operatorname{CC}) = |\mathcal{F}(h)|^2$. Therefore, we can obtain

$$h(t) = \mathcal{F}^{-1} \left(\pm \sqrt{\mathcal{F}[\operatorname{CC}(t)]} \right), \quad (\text{C1})$$

where the term \pm is understood to be applicable piecewise. Because the hill scale $\|h\|$ is arbitrary, we can simply assign $\operatorname{CC}(t) \leftarrow (g^{(2)}(t) - 1)$ and scale the resulting $h(t)$.

The existence of a precise solution depends on two conditions. The Fourier transform of the cross-correlation CC and the result $h(t)$ must both be non-negative. The positivity of the result can sometimes be ensured using a suitable piecewise sign-function \pm – a good example is a triangular CC resulting in a rectangular $h(t)$.

If the autocorrelation is given numerically, we can employ discrete Fourier transform (DFT) defined by relations

$$\text{DFT: } X_k = \sum_{n=0}^{N-1} x_n e^{-i2\pi nk/N}, \quad (\text{C2})$$

$$\text{DFT}^{-1}: x_n = \frac{1}{N} \sum_{k=0}^{N-1} X_k e^{i2\pi nk/N}. \quad (\text{C3})$$

Let us consider a given discrete series $\{c_n\} = c_0, c_1, \dots, c_{N-1}$ that defines the autocorrelation symmetrically around zero with a sampling interval δt ,

$$c_n := \operatorname{CC} \left[\left(n - \frac{N-1}{2} \right) \delta t \right]. \quad (\text{C4})$$

Then, we can approximate the Fourier transform

$$\begin{aligned} \widehat{\operatorname{CC}}(\nu) &= \int \operatorname{CC}(t) \exp(-i2\pi t\nu) dt \\ &\simeq \sum_n \operatorname{CC}(t_n) \exp(-i2\pi t_n \nu) \delta t, \end{aligned} \quad (\text{C5})$$

$$\begin{aligned} \widehat{c}_k &= \widehat{\operatorname{CC}} \left(\frac{k}{N\delta t} \right) \frac{1}{\delta t} \\ &= \text{DFT}(c_n) \exp \left(-i\pi \frac{N-1}{N} k \right). \end{aligned} \quad (\text{C6})$$

This way, we obtain the discrete Fourier transform with a sampling period $\delta\nu = 1/(N\delta t)$. We proceed and

get a discrete version of (C1).

$$h_m = \text{DFT}^{-1} \left((\pm 1)_k \sqrt{\hat{c}_k} \right) \frac{1}{\sqrt{\delta t}}. \quad (\text{C7})$$

If we consider the periodicity of DFT, we know that $h_m = h_{m-N}$ and we can map the implicit range $[0, N-1]$ to $[-(N-1)/2, (N-1)/2]$ and obtain the hill function

$$h(m \times \delta t) = \begin{cases} h_m & 0 \leq m \leq \frac{N-1}{2} \\ h_{m+N} & -\frac{N-1}{2} \leq m < 0 \end{cases}, \quad m \in \mathbb{Z}. \quad (\text{C8})$$

Appendix D: Derivation: non-overlapping hills

For high bunching, when the mean delay $\langle \Delta t \rangle = 1/\lambda$ is much greater than the width of the autocorrelation, the signal approaches a sequence of randomly distributed, but disjoint pulses $h(t)$. If a pulse generator is used, it cannot typically generate overlapping signals, which creates a distortion in the $g^{(2)}(\tau)$. If $h(t)$ is defined for $t \in (-t_0/2, t_0/2)$, the minimum delay Δt can be t_0 . This means that the peaks no longer follow a Poisson process, but a self-excited point process. The limitation of t_0 is akin to non-paralyzable dead time of particle detectors.

The distribution of peak pairs becomes more complicated. The term in (B7) that sums all the pairs needs to be evaluated separately for immediate neighbours, next-but-one neighbours, and so on. This is because the distribution $p_k(\Delta t)$ of $\Delta t_{i,i+k}$ must be calculated for each $k = 1, 2, 3, \dots$

$$\begin{aligned} \sum_{i < j} \text{CC}(\tau \pm \Delta t_{ij}) &= \sum_{k=1}^{N-1} \sum_{i=1}^{N-k} \text{CC}(\tau \pm \Delta t_{i,i+k}) \quad (\text{D1}) \\ &\simeq \sum_{k=1}^{N-1} (N-k) \langle \text{CC}(\tau \pm \Delta t) \rangle_{\Delta t \sim p_k} \end{aligned}$$

The first step is to consider the sequential delays $\Delta t_{i,i+1}$. By definition, these *are* independent realisations of a random Poisson process with an addition of t_0 . Therefore the probability density function is a shifted negative exponential

$$p_1(\Delta t) = \begin{cases} 0 & \Delta t < t_0 \\ \lambda e^{-\lambda(\Delta t - t_0)} & \Delta t \geq t_0 \end{cases}. \quad (\text{D2})$$

Now, considering that $\Delta t_{i,i+2} = \Delta t_{i,i+1} + \Delta t_{i+1,i+2}$, the constituent delays are mutually independent with known distributions. That means that the result has a known distribution. By further induction, as more independent terms are added, we can average over them in each step,

$$\begin{aligned} p_k(\Delta t) &= \int_{t'=0}^{\Delta t} p_{k-1}(t') p_1(\Delta t - t') dt' \\ &= \begin{cases} 0 & \Delta t < kt_0 \\ \lambda^k \frac{(\Delta t - kt_0)^{k-1}}{(k-1)!} e^{-\lambda(\Delta t - kt_0)} & \Delta t \geq kt_0 \end{cases}, \quad (\text{D3}) \end{aligned}$$

where Δt in p_k means $\Delta t_{i,i+k}$, describing its distribution over all i for $N \rightarrow \infty$.

As we assume the limit of long signals, but are interested in finite delays, let us fix τ and calculate the limit $N \rightarrow \infty$. After substitution of p_k into (D1), the averaged terms become

$$\begin{aligned} \langle \text{CC}(\tau \pm \Delta t) \rangle_{p_k} &= \int_{t=0}^{\infty} \text{CC}(\tau \pm t \pm kt_0) \\ &\quad \times \lambda^k \frac{t^{k-1}}{(k-1)!} e^{-\lambda t} dt. \quad (\text{D4}) \end{aligned}$$

Now let us recall that $\text{CC}(t)$ has a finite support and so for indices $k > |\tau|/t_0 + 1$, the first term $\text{CC}(\tau \pm t \pm kt_0) \equiv 0$ during the whole integration for both plus and minus signs. This means that for each finite τ , the number of non-zero terms in (D1) is finite. As a result, $k/N \rightarrow 0$ for each k . Also note that $T/N \rightarrow (1/\lambda + t_0)$. The result then is

$$\begin{aligned} g^{(2)}(\tau) &= \left(\frac{1}{\lambda} + t_0 \right) \sum_{k=1}^{|\lceil \tau \rceil / t_0 + 1} \int_{t=0}^{-(k-1)t_0 + |\tau|} \\ &\quad \times [C(\tau + t + kt_0) + C(\tau - t - kt_0)] \\ &\quad \times \lambda^k \frac{t^{k-1}}{(k-1)!} e^{-\lambda t} dt \\ &\quad + \left(\frac{1}{\lambda} + t_0 \right) C(\tau). \quad (\text{D5}) \end{aligned}$$

This result also trivially holds for the case when the minimum delay is t_0 , but the support of $h(t)$ is narrower. Moreover, the formula can also be adopted for the case of infinite support of $h(t)$ and $\text{CC}(t)$ with a minimum delay t_0 . In that case, both the sum and the integral would go to infinity; otherwise, the formula would be the same. The only difference in the derivation would be in proving the limit in (D1)

$$\lim_{N \rightarrow \infty} \sum_{k=1}^{N-1} \frac{k}{N} \langle \text{CC}(\tau \pm \Delta t) \rangle_k = 0. \quad (\text{D6})$$

As $\text{CC}(t)$ must be integrable, its tail scales faster than $1/t$. From (D4) and the integrability of the Gamma-like kernel, it follows that from a certain $k > k_0$, the term $\langle \text{CC}(\tau \pm \Delta t) \rangle_k$ decreases faster than $1/k$, which means that the limit of the series is zero.

Appendix E: Derivation: random switching of intensity levels

The signal $I(t)$ is now defined as a step function, where each intensity level I_i is held for a time period Δt_i . Each of these variables is independently governed by its probability density $p(I)$, $p(\Delta t)$. Let us denote averaging over these distributions by unmarked angle brackets $\langle \cdot \rangle$, where the distribution is determined by the random variable inside. Averaging over time will be marked by $\langle \cdot \rangle_t$. If we

denote the overall number of steps as N and the overall time as T , we get the mean intensity,

$$\begin{aligned} \langle I(t) \rangle_t &= \frac{1}{T} \sum_{i=1}^N \Delta t_i I_i = \frac{N}{T} \langle \Delta t I \rangle_t \\ &= \frac{1}{\langle \Delta t \rangle} \langle \Delta t \rangle \langle I \rangle = \langle I \rangle. \end{aligned} \quad (\text{E1})$$

This result easily follows from the uncorrelation of Δt and I . However, more discussion is needed for the auto-correlation term.

We express the integral as a sum over the steps again, but the term depends on the delay τ being greater/smaller than the step width Δt_i ,

$$\begin{aligned} \int_0^T I(t)I(t+\tau)dt &= \sum_i \begin{cases} (\Delta t_i - \tau) I_i^2 + \tau I_i I_i^{\text{eff}} & \Delta t_i > \tau \\ \Delta t_i I_i I_i^{\text{eff}} & \Delta t_i \leq \tau \end{cases}. \end{aligned} \quad (\text{E2})$$

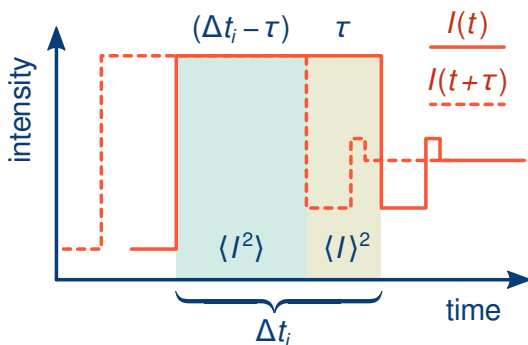


FIG. 5. The illustration of the integral overlap. The highlighted area marks the integration over the i -th step. After averaging, the two integral parts are revealed to correspond to the terms $\langle I^2 \rangle$ and $\langle I \rangle^2$.

The case of $\Delta t_i > \tau$ is illustrated in Fig. 5. The $\langle I^2 \rangle$ area on the left corresponds to the overlap where both signals have the intensity I_i . The $\langle I \rangle^2$ area on the right

is a product of $I(t) = I_i$ and the random intensity levels in $I(t + \tau)$ that follow the i -th level. We can express this integral overlap as $\tau I_i I_i^{\text{eff}}$, where I_i^{eff} is the average intensity of $I(t + \tau)$ in the area of width τ . If $\Delta t_i \leq \tau$, the i -th step has zero overlap with itself and only one term remains.

Now, if we consider the summation over i , we may again replace it with averaging over Δt and I independently. What is more, the variable I_i^{eff} gets averaged independently of I_i , because the intensity levels are mutually uncorrelated as well. Therefore $I_i^{\text{eff}} \rightarrow \langle I \rangle$, $I_i \rightarrow \langle I \rangle$, and $I_i^2 \rightarrow \langle I^2 \rangle$. However, the averaging over Δt needs to be split due to the piecewise definition in (E2). We obtain

$$\begin{aligned} \int_0^T I(t)I(t+\tau)dt &= N \int_{\tau}^{\infty} p(\Delta t) [(\Delta t - \tau) \langle I^2 \rangle + \tau \langle I \rangle^2] d\Delta t \\ &\quad + N \int_0^{\tau} p(\Delta t) \Delta t \langle I \rangle^2 d\Delta t. \end{aligned} \quad (\text{E3})$$

After extending the second integral to infinity to obtain the term $N \langle \Delta t \rangle \langle I \rangle^2$ and subtracting this extension from the integral on the left, we get

$$\begin{aligned} g^{(2)}(\tau) &= \frac{1}{T \langle I \rangle^2} \int_0^T I(t)I(t+\tau)dt \\ &= 1 + \frac{\langle I^2 \rangle - \langle I \rangle^2}{\langle \Delta t \rangle \langle I \rangle^2} \int_{\tau}^{\infty} p(\Delta t) (\Delta t - \tau) d\Delta t. \end{aligned} \quad (\text{E4})$$

FUNDING

- QuantERA ERA-NET Cofund in Quantum Technologies, EU Horizon 2020, and Ministry of Education, Youth and Sports of Czech Republic (Project HYPER-U-P-S, no. 8C18002)
- Czech Science Foundation (Grant 19-19189S)

[1] R. Loudon, *The Quantum Theory of Light*, third edition ed. (Oxford University Press, 2000).
 [2] W. Martienssen and E. Spiller, Coherence and Fluctuations in Light Beams, *American Journal of Physics* **32**, 919 (2005).
 [3] Y. Zhou, F.-l. Li, B. Bai, H. Chen, J. Liu, Z. Xu, and H. Zheng, Superbunching pseudothermal light, *Physical Review A* **95**, 053809 (2017).
 [4] J. S. Kim, Y. Huh, and M. W. Suh, A method to generate autocorrelated stochastic signals based on the random phase spectrum, *Journal of the Textile Institute* **101**, 471 (2010).
 [5] C. Müller, C. R. Rojas, and G. C. Goodwin, Generation

of amplitude constrained signals with a prescribed spectrum, *Automatica* **48**, 153 (2012).
 [6] B. Liu and D. Munson, Generation of a random sequence having a jointly specified marginal distribution and autocovariance, *IEEE Transactions on Acoustics, Speech, and Signal Processing* **30**, 973 (1982).
 [7] I. W. Hunter and R. E. Kearney, Generation of random sequences with jointly specified probability density and autocorrelation functions, *Biological Cybernetics* **47**, 141 (1983).
 [8] O. A. Z. Leneman, Correlation Function and Power Spectrum of Randomly Shaped Pulse Trains, *IEEE Transactions on Aerospace and Electronic Systems* **AES-3**, 774

- (1967).
- [9] D. Pandey, N. Satapathy, B. Suryabrahmam, J. S. Ivan, and H. Ramachandran, Classical light sources with tunable temporal coherence and tailored photon number distributions, *European Physical Journal Plus* **129**, 115 (2014).
- [10] I. Straka, J. Mika, and M. Ježek, Generator of arbitrary classical photon statistics, *Optics Express* **26**, 8998 (2018).
- [11] I. Straka and M. Ježek, Shaping the $g(2)$ autocorrelation and photon statistics, codeOcean (2020), DOI: [10.24433/CO.4221408.v1](https://doi.org/10.24433/CO.4221408.v1).
- [12] L. Mandel and E. Wolf, *Optical Coherence and Quantum Optics* (Cambridge University Press, 1995).
- [13] T. Kazimierczuk, J. Schmutzler, M. Aßmann, C. Schneider, M. Kamp, S. Höfling, and M. Bayer, Photon-Statistics Excitation Spectroscopy of a Quantum-Dot Micropillar Laser, *Physical Review Letters* **115**, 027401 (2015).
- [14] K. Yu. Spasibko, D. A. Kopylov, V. L. Krutyanskiy, T. V. Murzina, G. Leuchs, and M. V. Chekhova, Multiphoton Effects Enhanced due to Ultrafast Photon-Number Fluctuations, *Physical Review Letters* **119**, 223603 (2017).
- [15] D. Vasylyev, A. A. Semenov, and W. Vogel, Atmospheric Quantum Channels with Weak and Strong Turbulence, *Physical Review Letters* **117**, 090501 (2016).
- [16] D. Dravins, L. Lindgren, E. Mezey, and A. T. Young, Atmospheric intensity scintillation of stars, i. statistical distributions and temporal properties, *Publications of the Astronomical Society of the Pacific* **109**, 173 (1997).
- [17] M. Toyoshima, H. Takenaka, and Y. Takayama, Atmospheric turbulence-induced fading channel model for space-to-ground laser communications links, *Optics Express* **19**, 15965 (2011).
- [18] H. Shen, L. Yu, and C. Fan, Temporal spectrum of atmospheric scintillation and the effects of aperture averaging and time averaging, *Optics Communications* **330**, 160 (2014).
- [19] S.-K. Liao, W.-Q. Cai, J. Handsteiner, B. Liu, J. Yin, L. Zhang, D. Rauch, M. Fink, J.-G. Ren, W.-Y. Liu, Y. Li, Q. Shen, Y. Cao, F.-Z. Li, J.-F. Wang, Y.-M. Huang, L. Deng, T. Xi, L. Ma, T. Hu, L. Li, N.-L. Liu, F. Koidl, P. Wang, Y.-A. Chen, X.-B. Wang, M. Steindorfer, G. Kirchner, C.-Y. Lu, R. Shu, R. Ursin, T. Scheidl, C.-Z. Peng, J.-Y. Wang, A. Zeilinger, and J.-W. Pan, Satellite-Relayed Intercontinental Quantum Network, *Physical Review Letters* **120**, 030501 (2018).
- [20] J. Yin, Y.-H. Li, S.-K. Liao, M. Yang, Y. Cao, L. Zhang, J.-G. Ren, W.-Q. Cai, W.-Y. Liu, S.-L. Li, R. Shu, Y.-M. Huang, L. Deng, L. Li, Q. Zhang, N.-L. Liu, Y.-A. Chen, C.-Y. Lu, X.-B. Wang, F. Xu, J.-Y. Wang, C.-Z. Peng, A. K. Ekert, and J.-W. Pan, Entanglement-based secure quantum cryptography over 1,120 kilometres, *Nature* **582**, 501 (2020).